https://doi.org/10.5194/egusphere-2026-2824
Preprint. Discussion started: 16 June 2026
© Author(s) 2026. CC BY 4.0 License.

Three-dimensional atmospheric circulation teleconnections in the Northern Hemisphere

Haihong Yang[1], Shujuan Hu[1,2], Jianjun Peng[3] Wenxin Zhang[1], Zihan Hao[1], Yuchen Wu[1], and Zhiwei Zhu[4]

[1] College of Atmospheric Sciences, Lanzhou University, Lanzhou730000, China
[2] Collaborative Innovation Center for Western Ecological Safety, Lanzhou University, Lanzhou, China
[3] State Key Laboratory of Tropical Oceanography, South China Sea Institute of Oceanology, Chinese Academy of Sciences, Guangzhou, China
[4] State Key Laboratory of Climate System Prediction and Risk Management/Key Laboratory of Meteorological Disaster, Ministry of Education/Collaborative Innovation Center on Forecast and Evaluation of Meteorological Disasters, Nanjing University of Information Science and Technology, Nanjing 210044, China

Correspondence to: Shujuan Hu (hushuju@lzu.edu.cn)

Abstract. Atmospheric circulation teleconnections play a critical role in modulating low-frequency climate variability and driving regional extreme weather events, such as summer heatwaves. However, traditional teleconnection indices are predominantly defined using two-dimensional horizontal variables, which inadequately represent the dynamically crucial coupled vertical circulations. Here, we establish a three-dimensional analytical framework by applying the teleconnection method to the meridional and zonal vertical stream functions (H and W) derived from the three-pattern decomposition of global atmospheric circulation (3P-DGAC). We identify 14 structurally distinct vertical teleconnection patterns in the Northern Hemisphere mid-high latitudes, which demonstrate robust validity in reconstructing summer surface air temperature (SAT) and hemispheric circulation fields (yielding mean spatial correlations of 0.64 and 0.60, respectively, over 1979–2022). The proposed three-dimensional teleconnections effectively capture the low-frequency atmospheric variability that modulates Northern Hemisphere summer climate. Ultimately, this framework provides a unified dynamical perspective for understanding seasonal climate variability and offers a robust approach for diagnosing the atmospheric circulation mechanisms underlying regional temperature extremes.

https://doi.org/10.5194/egusphere-2026-2824
Preprint. Discussion started: 16 June 2026
© Author(s) 2026. CC BY 4.0 License.

1 Introduction

Atmospheric teleconnection patterns play a critical role in modulating summer climate variability across Eurasia and North America, exerting widespread impacts on socioeconomic systems through interconnected atmospheric processes (Affram et al., 2024; Ding et al., 2011; Ding and Wang, 2005; Folland et al., 2009; Li et al., 2019; Lu et al., 2002; Wu, 2002; Xu et al., 2019b, 2022; Yasunari et al., 2021; Zhu and Li, 2016). Beyond influencing large-scale climate variability, these patterns are recognized as primary drivers of regional climate extremes (Cassou et al., 2005; Enomoto et al., 2009; Huang et al., 2024; Liu et al., 2023; Tang et al., 2023; Thompson et al., 2019; Wulff et al., 2017; Xu et al., 2019a, 2020), simultaneously synchronizing climatic anomalies across geographically distant regions via atmospheric bridge mechanisms (Chen et al., 2016; Deng et al., 2018; Fu et al., 2024; Schubert et al., 2011, 2014; Xu et al., 2019b). Therefore, a comprehensive understanding of the structural dynamics of these teleconnection patterns is essential for enhancing the predictability of climate variability.

Previous studies have indicated that low-frequency atmospheric circulation variations are largely characterized by recurrent teleconnection patterns. Extensive investigations over the past decades have identified key patterns (Barnston and Livezey, 1987; Horel, 1981; Wallace and Gutzler, 1981), such as the Pacific-Japan (PJ) teleconnection pattern (Nitta, 1987), the Silk Road Teleconnection Wave Train (SRP) (Enomoto et al., 2003; Lu et al., 2002), the circumglobal teleconnection pattern (CGT) (Ding and Wang, 2005), the British-Baikal Corridor (BBC) and the British-Okhotsk Corridor (BOC) patterns (Xu et al., 2019b, 2022) among others. Recent advances have systematically characterized the properties of these hemispheric-scale patterns (Zheng and Wang, 2019). These patterns have shown significant utility in diagnosing synchronized extreme events across continents and enhancing subseasonal-to-seasonal prediction skills (Li and Ruan, 2018; Li et al., 2021; Lu and Lin, 2009; Wang et al., 2018, 2024; Zhu et al., 2023; Zhu and Li, 2016). Nevertheless, current diagnostic frameworks remain largely constrained by the two-dimensional nature of conventional circulation representations.

Traditionally, these predominantly horizontal circulation indices are derived from empirical orthogonal function (EOF) analyses or single-point correlation methods, which are limited in representing complete three-dimensional atmospheric structures. Specifically, conventional analyses primarily focus on horizontal components (e.g., geopotential height and horizontal stream function), often inadequately resolving the coupled vertical circulations that are crucial for a comprehensive three-dimensional perspective. This limitation restricts a holistic understanding of atmospheric low-frequency variability. However, observational and modeling evidence indicates that local vertical circulations dynamically interact with horizontal wave trains through coupled processes (Held and Phillips, 1990; Houze et al., 2000; Kiladis, 1998; Thakur et al., 2024). For instance, Kosaka and Nakamura (2006) highlighted the critical role of vertical flow structures in the development of meridional teleconnections. Furthermore, He et al. (2018) suggested that the sea ice-forced overturning vertical circulation triggers the formation of SRP. Therefore, to better capture three-dimensional atmospheric low-frequency variability, the recently developed three-pattern decomposition of global atmospheric circulation (3P-DGAC) is employed in this study. The 3P-DGAC addresses the limitations of traditional two-dimensional methods by synergistically decomposing horizontal, meridional, and zonal circulations on a global scale (Hu et al., 2017, 2018b, a, 2020). By utilizing this framework, we aim to systematically investigate the three-dimensional structures of teleconnections.

https://doi.org/10.5194/egusphere-2026-2824
Preprint. Discussion started: 16 June 2026
© Author(s) 2026. CC BY 4.0 License.

Given the pivotal role of vertical motion in the formation and evolution of atmospheric teleconnections, conceptualizing these patterns explicitly from the perspective of vertical circulation holds substantial dynamical significance. Building upon this foundation, this study extends the conventional concept of teleconnections by applying the teleconnection method (Wallace and Gutzler 1981) to vertical circulation stream functions derived from the 3P-DGAC, focusing on patterns that exhibit distinct three-dimensional structural features. Our results further suggest that these generalized teleconnection patterns may capture, at least partially, the essential characteristics of low-frequency atmospheric circulation variability in the Northern Hemisphere (NH). The findings provide a novel 3D perspective on the primary characteristics of atmospheric low-frequency variability, offering a theoretical basis for understanding the dynamic mechanisms behind large-scale summer temperature anomalies across the NH.

The remainder of this paper is organized as follows. Section 2 introduces the datasets and methodologies employed in this study. Section 3 outlines the definitions of vertical circulation teleconnection patterns and analyzes their three-dimensional structural characteristics. In Section 4, these established three-dimensional patterns are employed to reconstruct both summer surface temperature and large-scale circulation anomalies across the NH. Finally, Section 5 synthesizes the key findings, discusses their implications for climate dynamics, and proposes potential directions for future research.

2 Data and Methods

2.1 Datasets

This study utilizes the monthly reanalysis dataset from the European Centre for Medium-Range Weather Forecasts (ERA5; Hersbach et al. 2020), specifically extracting horizontal wind fields (u and v), geopotential height at multiple pressure levels, and 2 metre temperature (surface air temperature, SAT). The horizontal resolution is set at 2.5º × 2.5ºfor the period 1979–2022. Boreal summer is defined as the June–July–August (JJA) mean, and the climatology is based on the 1979–2010 reference period.

2.2 Methods

2.2.1 3P-DGAC

To better partition the three-dimensional structure of the global atmospheric circulation, this study adopts the 3P-DGAC framework (Hu et al. 2017, 2018a,b, 2020). This framework extends the classical concepts of mid-latitude Rossby waves and tropical Hadley-Walker circulations to formulate a unified representation of global horizontal, meridional, and zonal circulations. It not only quantitatively describes the large-scale horizontal circulation but also resolves the structures of local meridional and zonal vertical circulations, which are crucial components of atmospheric low-frequency variability. By utilizing the 3P-DGAC, this study systematically extracts vertical circulation teleconnection patterns—features often underrepresented in traditional two-dimensional decompositions—thereby extending the analysis to three-dimensional structures.

By inputting the global horizontal wind fields (u and v) into the 3P-DGAC model, the three-dimensional stream functions (R, H, and W) for the horizontal, meridional, and zonal circulations are obtained. By inverting the relationship between the stream functions and the velocity fields, six velocity components corresponding to the

https://doi.org/10.5194/egusphere-2026-2824
Preprint. Discussion started: 16 June 2026
© Author(s) 2026. CC BY 4.0 License.

decomposed circulations are derived. Namely, we have the horizontal velocities u_R and v_R of horizontal circulation, the north-south horizontal velocity v_H and vertical velocity ω_H of meridional circulation, and the east-west horizontal velocity u_W and vertical velocity ω_W of zonal circulation. The specific calculation procedures are referred to the references(Hu et al., 2017, 2018a, b). and the Supplementary Material.

2.2.2 Stepwise regression analysis.

Stepwise regression is a multiple linear regression approach that identifies the optimal combination of independent variables via iterative forward selection and backward elimination (Deng et al., 2019). This iterative feature makes stepwise regression particularly useful for mitigating multicollinearity when independent variables are highly correlated (Taylor et al., 1998). In this study, a stepwise regression model is employed to quantify the relative contributions of various atmospheric circulation patterns to natural SAT anomalies in the NH. Natural SAT anomalies are isolated by linearly detrending the raw SAT data to approximate and remove the background global warming signal (Henley et al., 2015). The detailed calculation steps are outlined below (Zheng and Wang, 2019):

1) Fit the initial model.

2) Add the term with the lowest P-value. If no term in the model has an F-statistic P-value below the entry threshold, repeat this step; otherwise, move on to step 3.

3) If any term in the model has an F-statistic P-value exceeding the exit threshold, remove the term with the highest P-value and return to step 2; otherwise, conclude the process.

2.2.3 Attribution analysis based on stepwise regression analysis.

First, the SAT variations explained by global warming (SAT_{gw}) are estimated as difference between the raw SATs and detrended SATs. Then, by the stepwise regression model, the portion of SAT changes explained by atmospheric circulation patterns (SAT_{acp}) is defined as the value of the terms associated with the given circulation patterns in the regression equation. The portion of SAT changes that cannot be explained by either atmospheric circulation patterns or global warming is defined as the residual SAT (SAT_{res}). Finally, based on these definitions, we calculated the contribution rate C of global warming and atmospheric circulation patterns to SAT changes, as follows:

$$C = \left(\left|SAT_{gw}\right| + \left|SAT_{acp}\right|\right) / \left(\left|SAT_{gw}\right| + \left|SAT_{acp}\right| + \left|SAT_{res}\right|\right). \quad (1)$$

Here, $\left|SAT\right|$ represents the absolute value of SAT.

2.2.4 Reconstruction of circulation anomalies.

The NH circulation patterns for specific target years were reconstructed using the following protocol.

1) Year-specific anomaly identification. For a given target year y, a threshold of ±1 standard deviation of the predefined teleconnection indices is utilized to identify the dominant anomalous circulation patterns. These relative anomaly

https://doi.org/10.5194/egusphere-2026-2824
Preprint. Discussion started: 16 June 2026
© Author(s) 2026. CC BY 4.0 License.

circulation patterns are referred to as: $HP\text{-}Tel_{y1}, HP\text{-}Tel_{y2}, ..., HP\text{-}Tel_{yn}$, where n represents the total number of circulation patterns identified as anomalous for a given target year y.

2) Index-weighted reconstruction. The reconstructed circulation field (Recon_Ciry) for year y is linearly combined as follows:

$$Recon\_Cir_y = \sum_{i=1}^{n} TI_{yi} \times HP\text{-}Tel_{yi} \quad (2)$$

Where TIyi denotes the index of the i-th anomalous horizontal circulation patterns (HP-Teli) for a given target year y, with its precise definition provided in Eq. (5) and Eq. (6).

3. Results

3.1 New definitions of meridional and zonal vertical circulation teleconnections.

Here, we apply the teleconnection method (Wallace and Gutzler, 1981) to the stream function H(or W) of meridional (or zonal) vertical circulation derived from the 3P-DGAC model, identifying several vertical circulation teleconnection patterns in the NH mid-high latitudes during summer (180°W–180°E, 25°–90°N) (Fig. 1).

Specifically, for the meridional vertical circulation patterns (the approach for the zonal vertical circulation is analogous), the correlation coefficient r_{ij} between the time series of stream function anomalies H_i at grid point i and H_j at grid point j on the 500 hPa isobaric surface are calculated as follows:

$$r_{ij} = \frac{\sum_{t=1}^{L}(H_i(t)-\overline{H_i})(H_j(t)-\overline{H_j})}{\sqrt{\sum_{t=1}^{L}(H_i(t)-\overline{H_i})^2}\sqrt{\sum_{t=1}^{L}(H_j(t)-\overline{H_j})^2}}. \quad (3)$$

Where L denotes the length of the time series and t denotes time index, ranging from 1 to L. $\overline{H_i}$ (or $\overline{H_j}$) represents the average value of $H_i(t)$ (or $H_j(t)$).

For each grid point i, the strongest negative correlation coefficient is extracted as:

$$T_i = \min_{1<j<N}(r_{ij}), \quad (4)$$

where N denotes the total number of grid points. By compiling these strongest negative correlation coefficients T_i across all grid points i, we construct the teleconnectivity matrix T for the 500-hPa meridional stream function H (and similarly for the zonal stream function W). Statistically significant teleconnections (at the 99.99% confidence level) are identified as paired endpoints in matrix T, where the connecting lines illustrate remote meridional (or zonal) circulation linkages (Fig. 1).

Furthermore, to quantitatively characterize the temporal variations of these patterns, the teleconnection indices for the meridional and zonal vertical circulations are defined as follows:

https://doi.org/10.5194/egusphere-2026-2824
Preprint. Discussion started: 16 June 2026
© Author(s) 2026. CC BY 4.0 License.

$$TI_H = (H_A - H_B)/2, \quad (5)$$

$$TI_W = (W_A - W_B)/2, \quad (6)$$

where H_A (or W_A) and H_B (or W_B) represent the stream function anomalies at endpoints A and B, respectively, serving as an indicator of the teleconnection intensity.

Through a systematic analysis of the meridional stream function (H) teleconnectivity matrix during summers from 1979 to 2022, seven statistically significant meridional vertical teleconnection patterns are identified across the NH mid-latitudes (Fig. 1a; Table S1). These patterns are geographically designated as the Polar I (HP), Canadian-Bermuda (HCB), Caspian Sea-Tarim (HCST), Central Siberia-Kara Sea (HSK), Greenland-Scandinavia (HGS), Black Sea-Aleutian (HBA), and Ural-Baltic (HUB) patterns, where the prefix 'H' denotes the meridional stream function. To elucidate their physical manifestations, the meridional stream function H is regressed onto each pattern's index. The results reveal coupled counter-rotating cells along meridional cross-sections at the endpoints, manifesting as zonally aligned dipole pairs spanning the hemisphere (Fig. S1). These paired vertical cells constitute distinct vertical teleconnections, as exemplified by the counter-rotating cells of the HCB pattern over the Canadian Plains and Bermuda, with similar dipole structures observed across the other patterns (Fig. S1). Similarly, seven zonal vertical teleconnections are identified from the teleconnectivity matrix of the zonal stream function (W). These are designated as the Polar II (WP), Mongolia-Central Siberia (WMCS), West Siberian-Junggar (WWSJ), Greenland Sea-Azores (WGA), Ogasawara-Mexico (WOM), Chukchi Sea-Victoria (WCV), and Bering Strait-Aleutian (WBA) patterns, with the prefix 'W' indicating the zonal stream function (Fig. 1b; Table S2). These zonal teleconnections feature meridionally aligned counter-rotating zonal cells (Fig. S2), contrasting with the zonal orientation of the meridional patterns. The WMCS pattern exemplifies this structure, exhibiting counter-rotating zonal cells over the Mongolian and West Siberian plateaus—a configuration broadly representative of the other zonal patterns.

These findings highlight the existence of distinct meridional and zonal vertical teleconnections, expanding upon traditional two-dimensional paradigms and providing new insights into atmospheric circulation variations.

https://doi.org/10.5194/egusphere-2026-2824
Preprint. Discussion started: 16 June 2026
© Author(s) 2026. CC BY 4.0 License.

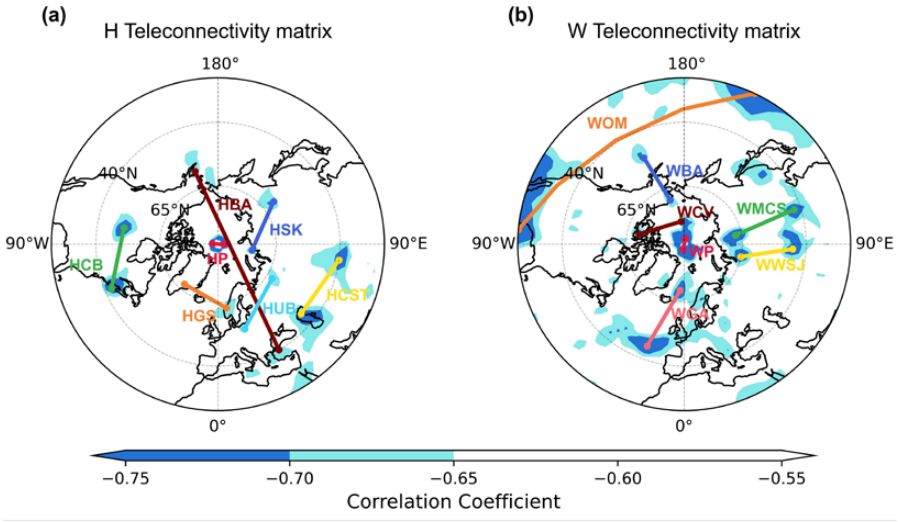

Figure 1. Teleconnectivity map of vertical circulation. (a) Teleconnectivity map of summer 500-hPa stream function H of meridional circulation and (b) stream function W of zonal circulation in the NH for the period of 1979–2022. The data are detrended before analysis, and the areas where the strongest negative correlation coefficients are less than –0.65 are shaded. The teleconnection lines, which connect two grid points having the strongest negative correlation with each other ($\alpha \leq 0.01\%$), are plotted on the teleconnectivity map to reveal atmospheric circulation patterns. The atmospheric circulation patterns found by this study in (a) are Polar I pattern (HP), Canadian-Bermuda pattern (HCB), Caspian Sea-Tarim pattern (HCST), Central Siberia-Kara sea pattern (HSK), Greenland-Scandinavia pattern (HGS), Black Sea-Aleutian pattern (HBA), and Ural-Baltic pattern (HUB).The atmospheric circulation patterns found by this study in (b) are Polar II pattern (WP), Mongolia-Central Siberia pattern (WMCS), West Siberian-Junggar pattern (WWSJ), Greenland Sea-Azores pattern (WGA), Ogasawara-Mexico pattern (WOM), Chukchi Sea-Victoria pattern (WCV), and Bering Strait-Aleutian pattern (WBA).

3.2. Three-dimensional circulation teleconnection patterns.

To capture the horizontal circulation signatures associated with these vertical teleconnections, the 200-hPa geopotential height (GHT) anomalies are regressed onto the respective vertical circulation indices. The resultant horizontal regression patterns corresponding to the 14 vertical teleconnections are designated as the HP-series (HP standing for "horizontal pattern"), as shown in Fig. 2.

Certain horizontal circulation patterns associated with the meridional vertical teleconnections (HP-H series) manifest classical wave train signatures across the NH (Fig. 2). For instance, the HP-HCB exhibits a zonal wave train spanning from the northeastern Pacific to the western Atlantic (Fig. 2b). The HP-HCST displays a mid-latitude Eurasian wave train with anomaly centers over Eastern Europe, Western Asia, and Central Asia (Fig. 2c), which is structurally consistent with the Silk Road Pattern (SRP) ($r = 0.89$, $p < 0.01$; Fig. S3). The four-center structure of the HP-HSK, extending from Britain to Lake Baikal (Fig. 2d), closely mirrors the British-Baikal Corridor (BBC) pattern ($r = -0.77$, $p < 0.01$; Fig. S4). The HP-HUB exhibits positive anomalies over the British Isles and northern Siberia contrasting with negative anomalies over western Russia (Fig. 2b), resembling the British-Okhotsk Corridor pattern ($r = 0.74$, $p < 0.01$; Fig. S5). S Similarly, the horizontal circulation patterns linked to the seven zonal vertical teleconnections (the HP-W series) demonstrate distinctive regional signatures. The HP-WMCS exhibits a meridional dipole spanning from Greenland to Siberia (Fig. 2i), whereas the HP-WWSJ shows a tripole structure across Greenland, Europe, and Siberia

https://doi.org/10.5194/egusphere-2026-2824
Preprint. Discussion started: 16 June 2026
© Author(s) 2026. CC BY 4.0 License.

(Fig. 2j). Notably, the North Atlantic dipole pattern exhibited by the HP-WGA (Fig. 2k) aligns closely with the summer North Atlantic Oscillation (NAO) pattern (Greatbatch and Rong 2006).

The analysis demonstrates that the horizontal patterns associated with these vertical teleconnections encompass many of the well-documented NH low-frequency modes (e.g., SRP, BBC, summer NAO). This consistency suggests that the proposed vertical circulation framework effectively captures key low-frequency variability patterns in the NH summer circulation. Hence, it serves as a robust approach for identifying essential atmospheric circulation characteristics. Furthermore, this approach identifies several patterns not heavily emphasized in previous conventional analyses (e.g., HP-WMCS, HP-WGA, HP-WOM), potentially offering new insights into the atmospheric dynamics linked to extreme weather events. Additionally, this framework supports the utility of 3P-DGAC stream functions for teleconnection analysis and enables the systematic comparison of previously identified modes within a unified three-dimensional perspective.

https://doi.org/10.5194/egusphere-2026-2824
Preprint. Discussion started: 16 June 2026
© Author(s) 2026. CC BY 4.0 License.

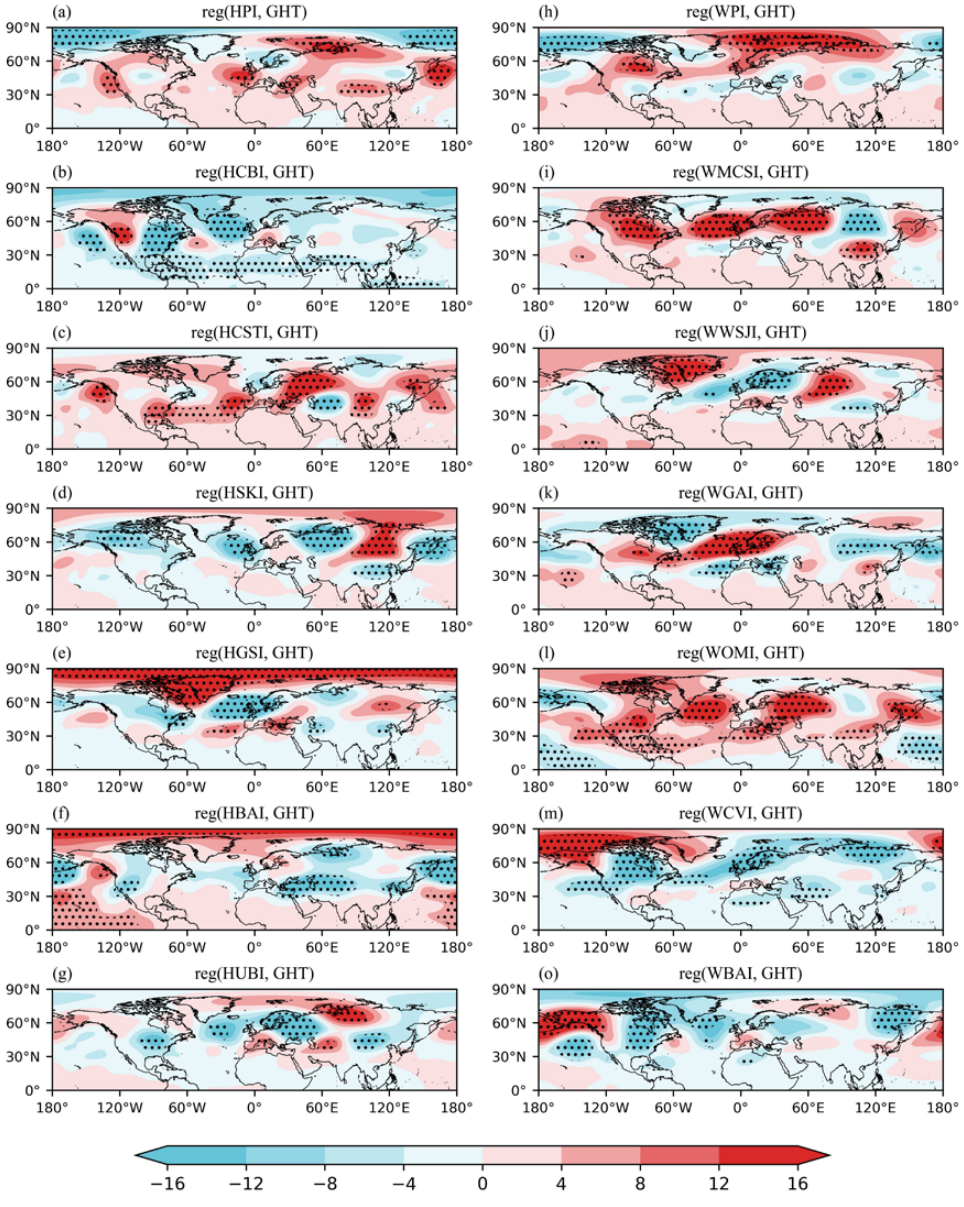

Figure 2. Horizontal spatial structure of atmospheric circulation patterns. (a)–(g) Regressed summer 200-hPa GHT anomalies(shading units: gpm) onto HPI, HCBI, HCSTI, HSKI, HGSI, HBAI, and HUBI for the period of 1979–2022. (h)–(n) As in (a)–(g), but for WPI, WMCSI, WGAI, WOMI, WWSJI, WCVI, and WBAI. Data are detrended prior to analysis, and dotted areas indicates results significant at the 95% confidence level.

Then, to elucidate the coupling mechanisms between horizontal circulation patterns and vertical cells, we constructed horizontal distributions of regressed stream function H (W) at 500 hPa (Fig. 3a–f), and meridional (zonal) cross-sections across key anomaly centers (Fig. 3g–z2). Three-dimensional circulation analysis reveals synchronized

https://doi.org/10.5194/egusphere-2026-2824
Preprint. Discussion started: 16 June 2026
© Author(s) 2026. CC BY 4.0 License.

225 horizontal wave trains and vertical cells between pressure systems (Fig. 3-4). Specifically, the ascending (descending) branches of these vertical circulation cells are situated ahead of cyclones (anticyclones) and behind anticyclones (cyclones), consistent with the constraints of the omega equation within the quasi-geostrophic framework at mid-to-high latitudes (Xu et al., 2019b). This indicates that vertical motion remains a crucial factor in the development of various weather phenomena (Pendergrass and Gerber, 2016; Sardeshmukh et al., 2015; Tamarin-Brodsky and Hadas,
230 2019), occupying a significant role in atmospheric circulation evolution.

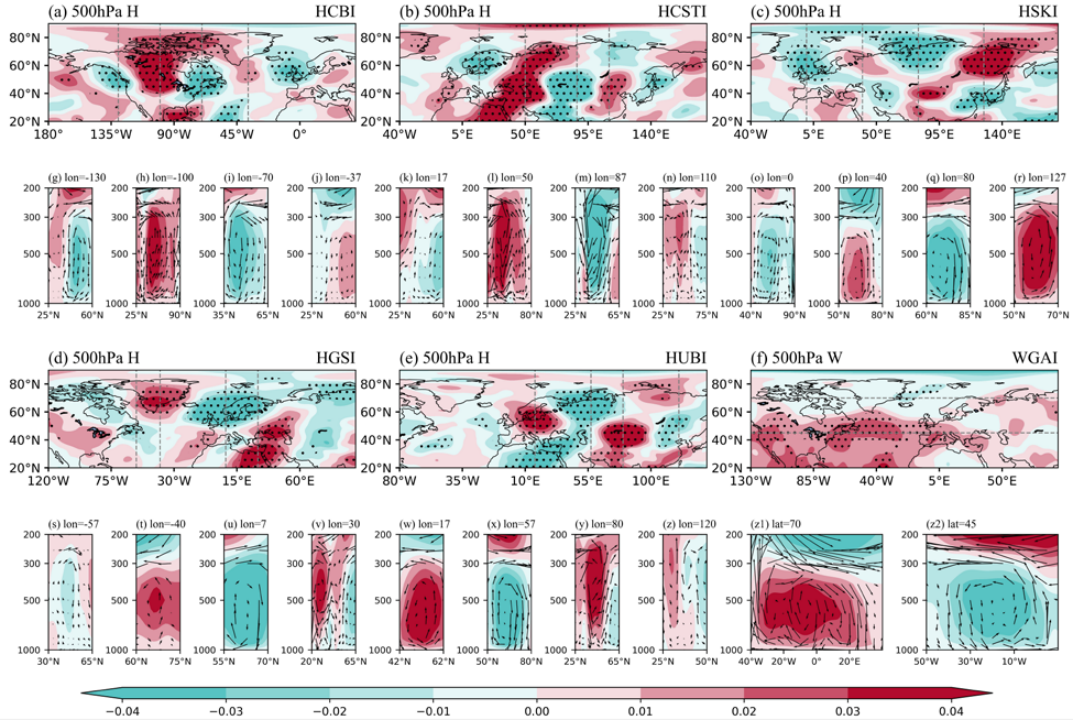

Figure 3. Three-dimensional circulation structure of the teleconnection patterns. (a)–(e) Regressed summer 500 hPa stream function H anomalies(shading units:10-6m-1) onto HPI, HCBI, HCSTI, HSKI and HGSI. (f) Regressed summer 500 hPa stream function W anomalies(shading units:10-6m-1) onto WGAI. The areas with the significant at the 95% confidence
235 **level are dotted. Meridional cross-section of the anomalous center of the regression field of the 500 hPa stream function H (Regressed onto the (g)–(j) HCBI, (k)–(n) HCSTI, (o)–(r) HSKI, (s)–(v) HGSI and (w)–(z) HUBI). (z1)–(z2): Zonal cross-section of the anomalous center of the regression field of the 500-hPa stream function W (Regressed onto the WGAI).**

https://doi.org/10.5194/egusphere-2026-2824
Preprint. Discussion started: 16 June 2026
© Author(s) 2026. CC BY 4.0 License.

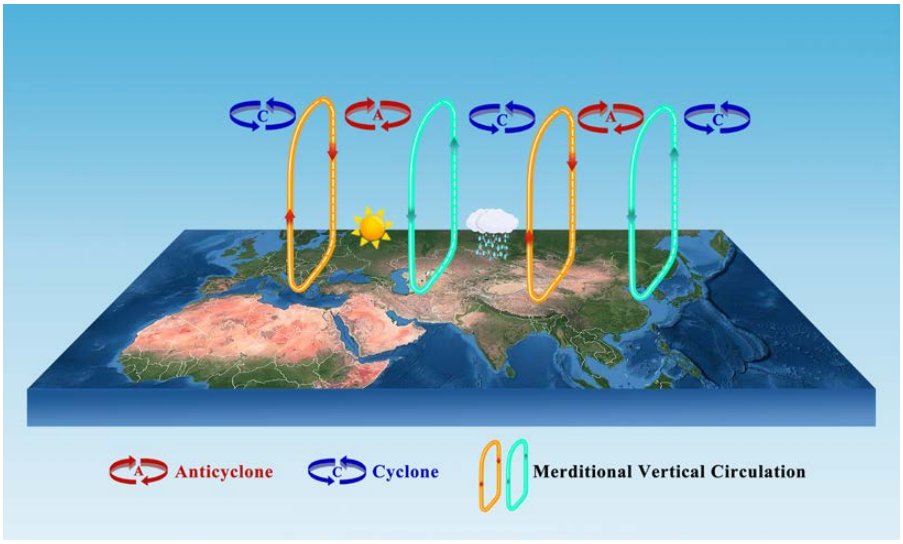

Figure 4. Mechanism diagram of Three-dimensional circulation teleconnection patterns.

Collectively, these analyses suggest that investigations into the formation, development, and impacts of horizontal teleconnections should simultaneously account for the coupled vertical circulation patterns. Previous studies have generally categorized teleconnections into zonally symmetric modes (e.g., the Hadley circulation) and zonally asymmetric modes (e.g., the Pacific-North American pattern) (Liu and Alexander, 2007). Our findings imply a dynamical connection between these two types of teleconnections and propose that the traditionally emphasized two-dimensional horizontal teleconnection paradigm should be broadened to encompass a fully three-dimensional structural framework. This offers new insights and alternatives for the study of teleconnection patterns. This expanded framework offers new insights and perspectives for diagnosing atmospheric teleconnections.

3.3 Integrated Modulation of Climate Variability by Three-Dimensional Atmospheric Circulation Patterns.

Previous studies have demonstrated a robust correspondence between large-scale SAT and GHT anomalies during summer, wherein positive GHT anomalies generally co-occur with warm SAT anomalies, and vice versa (Fu et al., 2025; Lembo et al., 2024; Li et al., 2021; Tang et al., 2023; Wang et al., 2022; Xu et al., 2019b; Zhang et al., 2023). As discussed in the preceding section, the identified three-dimensional circulation patterns effectively capture the key modes of low-frequency atmospheric circulation variability in the NH. To further assess the utility of these three-dimensional patterns in diagnosing large-scale climate variability, we now focus on their relationship with NH SAT anomalies. Specifically, the 14 newly defined atmospheric circulation indices are utilized to reconstruct the observed SAT anomalies. Furthermore, to demonstrate the robustness of this framework, we also reconstruct the associated large-scale atmospheric circulation anomalies using these dominant circulation indices.

3.3.1 Contribution of three-dimensional teleconnections to NH temperature variance.

Recent NH heatwaves have highlighted the critical role of anomalous circulation patterns in driving SAT extremes (Huang et al., 2024; Tang et al., 2023; Zhang et al., 2023; Zheng and Wang, 2019). To systematically quantify the

https://doi.org/10.5194/egusphere-2026-2824
Preprint. Discussion started: 16 June 2026
© Author(s) 2026. CC BY 4.0 License.

temperature modulation associated with individual circulation patterns, SAT anomalies are regressed onto the respective circulation indices (Fig. 5). The regression analysis indicates that these patterns exert significant modulating effects on the SAT field. Specifically, the HP-HCB is associated with alternating warm and cold anomalies across mid-latitude North America (Fig. 5b), whereas the HP-WMCS is linked to concurrent warming over Canada and western Siberia, accompanied by cooling in central Siberia (Fig. 5i). Overall, the anomaly centers of these circulation patterns closely align with the SAT anomaly centers (Fig. 5), reflecting the strong coupling between these circulation modes and the NH summer SAT.

Moreover, each identified horizontal circulation pattern exhibits a unique spatial configuration, which corresponds to a distinct spatial distribution of SAT anomalies. Consequently, the observed large-scale SAT anomalies across the NH are typically modulated by the combined effects of multiple concurrent circulation patterns (Zheng and Wang, 2019). As demonstrated above, these horizontal circulation patterns—anchored by vertical teleconnections—exhibit varying degrees of influence on the NH SAT. To quantitatively evaluate their collective contribution to the hemispheric temperature variability, the summer SAT anomalies for 1979–2022 are reconstructed using a stepwise regression of the teleconnection indices. This approach effectively mitigates multicollinearity issues while isolating the dominant circulation modes that modulate SAT variability.

The reconstructed SAT anomalies exhibit high consistency with observations, yielding a 43-year mean spatial correlation of 0.64 (Fig. S6). Particularly during extreme heat years (e.g., 2016, 2018, 2019, 2021, and 2022), the spatial correlations exceed 0.75, highlighting the robust capability of these patterns in reproducing hemispheric-scale temperature extremes (Figs. S7–S10).

https://doi.org/10.5194/egusphere-2026-2824
Preprint. Discussion started: 16 June 2026
© Author(s) 2026. CC BY 4.0 License.

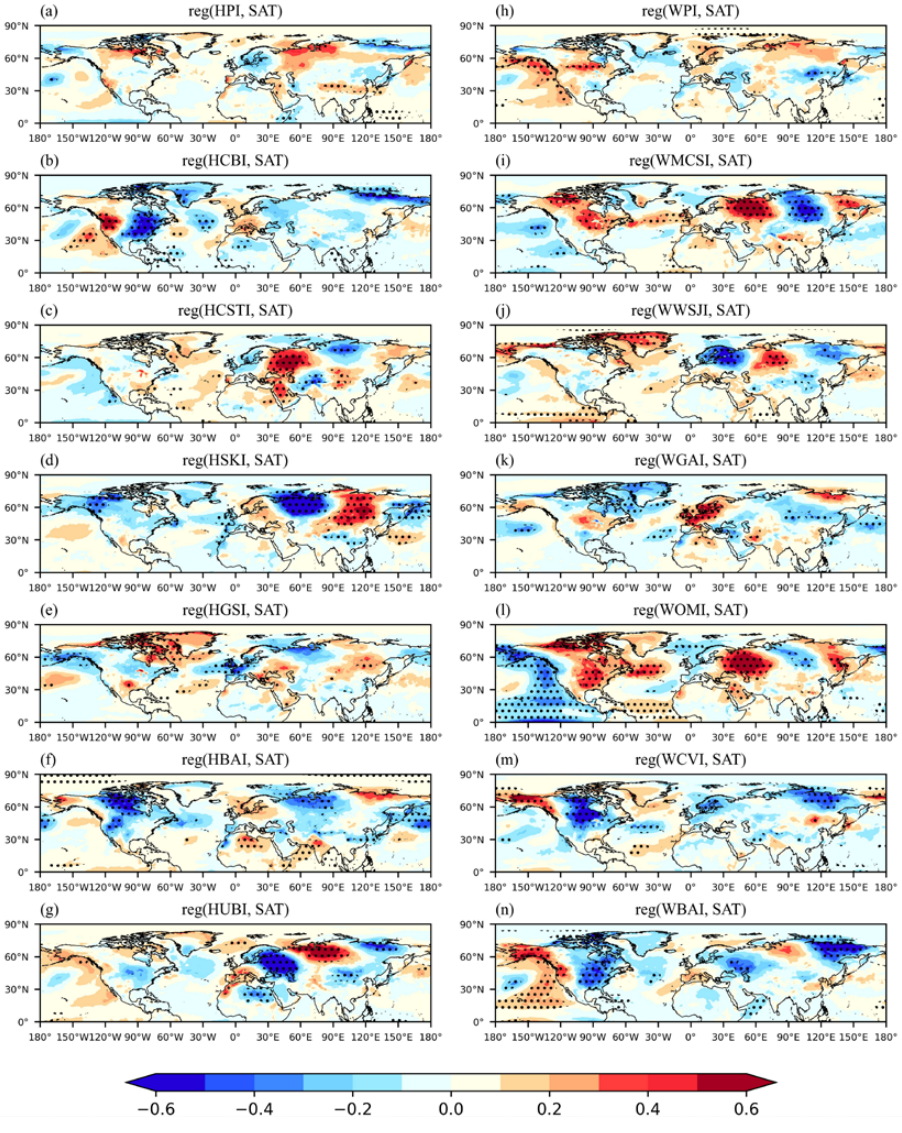

Figure 5. Summer SAT variations in association with the atmospheric circulation patterns. (a)–(g) Regressed summer mean T2M anomalies (shading units: °C) onto HPI, HCBI, HCSTI, HSKI, HGSI, HBAI, and HUBI for the period of 1979-2018. (h)–(n) As in (a)–(g), but for WPI, WMCSI, WGAI, WOMI, WWSJI, WCVI, and WBAI. The data are detrended before analysis, and the areas with the significant at the 95% confidence level are dotted.

Notably, the 2022 case exhibits substantial explanatory power, with the circulation patterns accounting for 56% of the SAT variance across the hemisphere (Fig. 6). Specifically, the western United States, northern Europe, and southern China exhibited severe positive temperature anomalies (Fig. 6a). Based on the stepwise regression analysis, the combined contributions of the global warming trend and atmospheric circulation patterns to the SAT anomalies in the western United States, northern Europe, and southern China are 77.20%, 80.00%, and 81.20%, respectively (Fig. 6c). This indicates that the SAT variations in these regions are largely modulated by the identified atmospheric circulation

https://doi.org/10.5194/egusphere-2026-2824
Preprint. Discussion started: 16 June 2026
© Author(s) 2026. CC BY 4.0 License.

patterns. For instance, the SAT anomalies in the western United States are primarily modulated by the HP-HBA, HP-WP, and HP-HCB. Therefore, the proposed circulation framework effectively captures summer temperature variations across both typical and extreme years, at both hemispheric and regional scales. These results suggest that a better representation of these low-frequency atmospheric circulation modes could enhance the predictability of summer SAT in the NH.

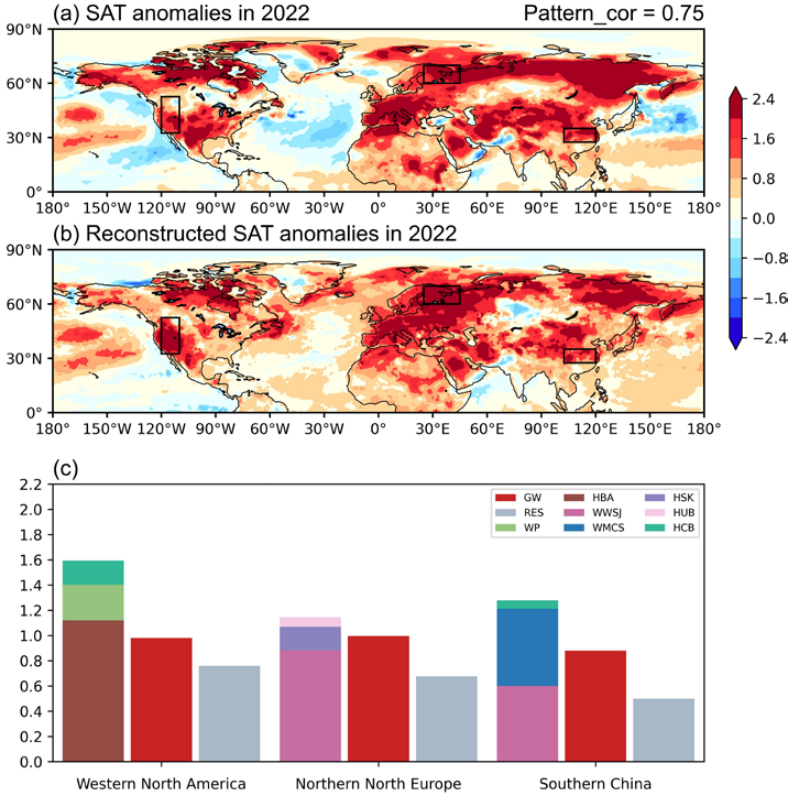

Figure 6. Combined effect of global warming and atmospheric circulation patterns on summer SAT. (a) SAT anomalies (shading, units: °C) in the NH during the summers of 2022. (b) Reconstructed summer SAT anomalies (shading, units: °C) in the NH during the summers of 2022. (c) Attribution analyses of the SAT variations (units: °C) in the west of North America (120°–110°W, 32.5°–52.5°N), northern Europe (25°–45°E, 60°–70°N), and Southern China (102.5°–120°E, 27.5°–35°N) during the summer of 2022. GW is abbreviation for global warming.

3.3.2 Dominant teleconnection patterns modulating large-scale SAT anomalies in the NH.

Although the grid-point SAT reconstruction demonstrates the utility of these patterns in explaining climate variability, it does not explicitly account for the spatial coherence of the atmospheric circulation. The increasing frequency of extreme heatwaves, such as the 2022 event, underscores the need to understand their large-scale dynamic drivers. Therefore, we investigate the effectiveness of the identified horizontal circulation patterns in reconstructing large-scale circulation anomalies, using the summer of 2022 as a case study.

As shown in Fig. 7, five circulation patterns (HP-WWSJ, HP-WMCS, HP-HP, HP-HBA, and HP-WGA) are identified as potential contributors to the circulation anomalies in 2022. A robust analysis requires evaluating both the individual

https://doi.org/10.5194/egusphere-2026-2824
Preprint. Discussion started: 16 June 2026
© Author(s) 2026. CC BY 4.0 License.

pattern amplitudes and their relative magnitudes. Among the 14 teleconnection indices in 2022, the WWSJI, WMCSI, and HPI exceeded one standard deviation (Fig. 8a). Therefore, these three patterns represent the dominant active modes during that summer. Following the established methodology, the 200-hPa geopotential height anomalies are reconstructed through a linear combination of these dominant patterns. T The reconstructed circulation anomalies (Fig. 8c) exhibit a spatial correlation of 0.74 with the observations (Fig. 8b), successfully reproducing key features such as the positive anomalies over the North Atlantic and Ural mountains, and the negative anomalies over Greenland and Siberia. Notably, the HP-WWSJ is the dominant contributor to this reconstructed field, and these patterns represent modes that have not been extensively characterized in previous studies. This provides a dynamical context for the occurrence of concurrent heatwaves across the NH in 2022. Furthermore, the reconstruction framework demonstrates robust performance across other extreme years (e.g., 2016 and 2018), as detailed in the Supporting Information (Figs. S11–S12), supporting its generalizability beyond a single event.

When applied to the full 1979–2022 period, the reconstructed circulation fields maintain high consistency with the observational data, yielding an average spatial correlation coefficient of 0.60 (Fig. S6). In conclusion, two independent lines of evidence converge to support our central finding: both (1) the reconstruction of grid-point temperature anomalies, which does not consider the structural integrity of circulation patterns, and (2) the reconstruction of hemispheric circulation anomalies, which incorporates the holistic spatial characteristics and anomaly magnitudes, jointly demonstrate that the horizontal circulation patterns defined in this study robustly capture the essential features of low-frequency atmospheric variability. The identification of these three-dimensional circulation patterns contributes to a more comprehensive understanding of large-scale climate variability in the NH. Therefore, an improved representation of the emergence and intensity of these three-dimensional circulation patterns holds practical significance for forecasting summer surface temperatures.

https://doi.org/10.5194/egusphere-2026-2824
Preprint. Discussion started: 16 June 2026
© Author(s) 2026. CC BY 4.0 License.

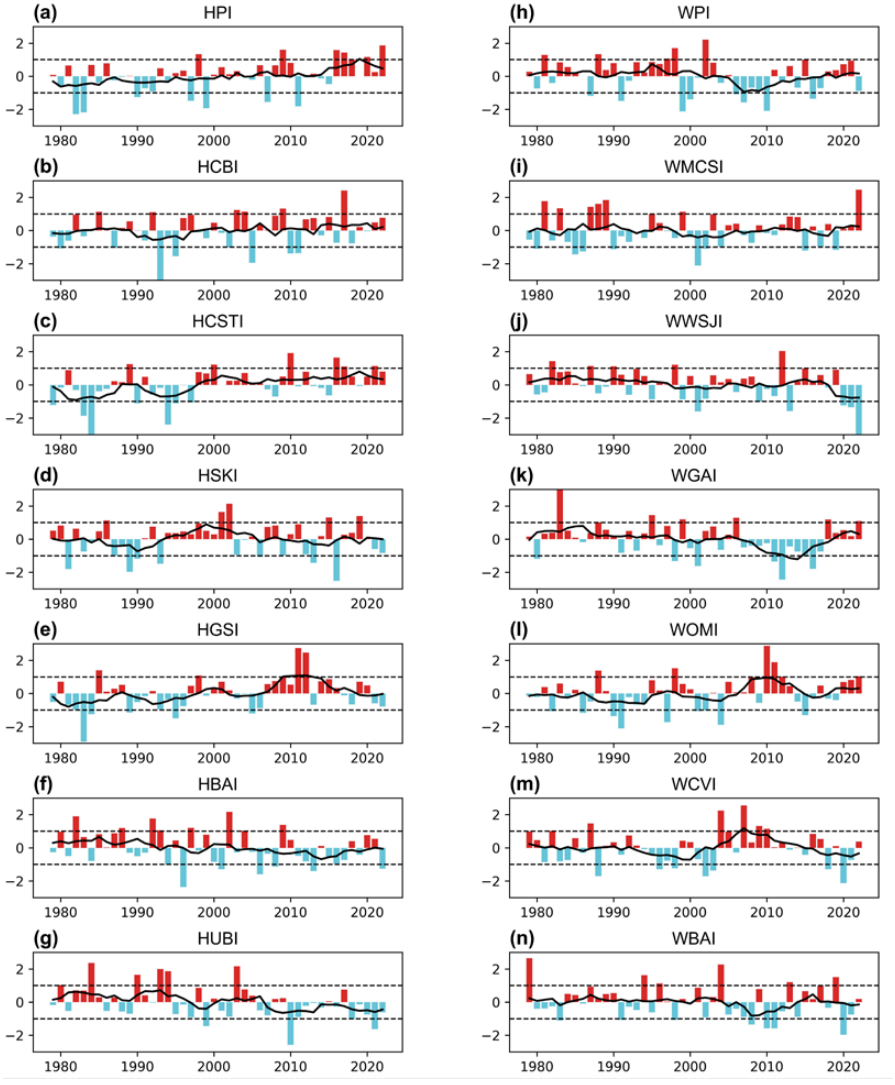

Figure 7. Time series of Teleconnection patterns. (a)–(g) Standardized time series of HPI, HCBI, HCSTI, HSKI, HGSI, HBAI, and HUBI (bar) and their seven-year running mean (black line) for the period of 1979–2022. (h)–(n) Same as (a)–(g), but for WPI, WMCSI, WGAI, WOMI, WWSJI, WCVI, and WBAI. The dashed lines denote the reference line of ±1 standard deviation.

https://doi.org/10.5194/egusphere-2026-2824
Preprint. Discussion started: 16 June 2026
© Author(s) 2026. CC BY 4.0 License.

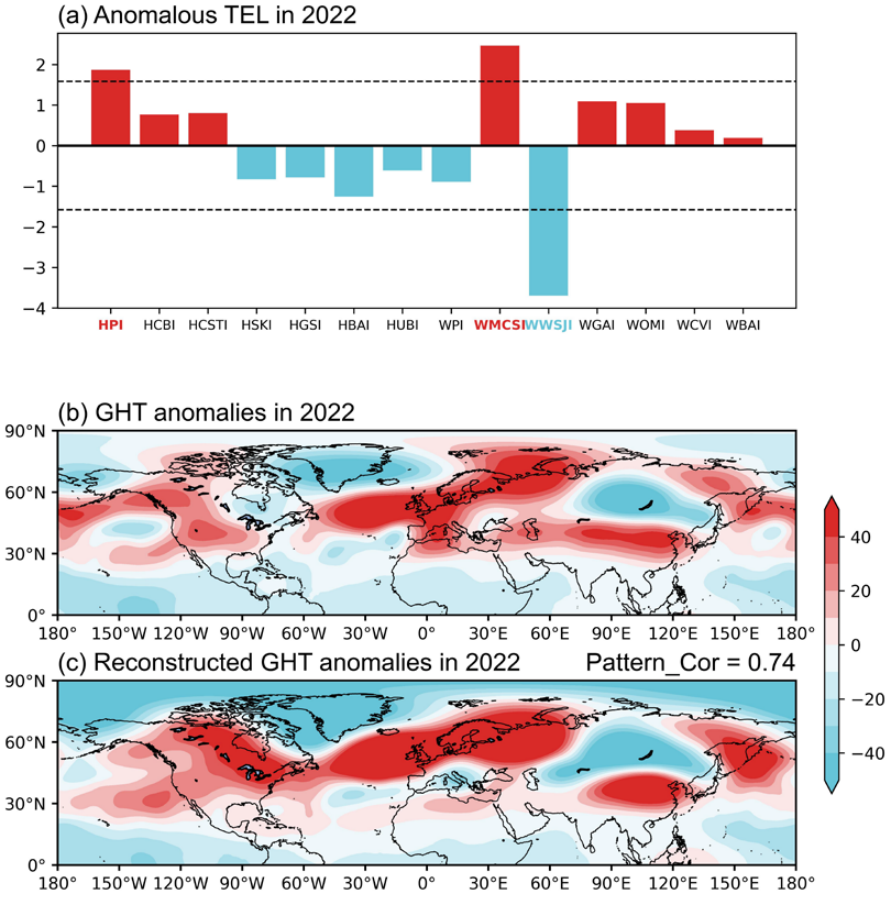

Figure 8. Reconstructed circulation anomalies in 2022. (a) Indices of teleconnection patterns in 2022. The dashed lines denote the reference line of the ± 1 standard deviation. (b) Summer GHT anomalies (shading, units: gpm) in the NH during the summer of 2022. (c) Reconstructed Summer GHT anomalies (shading, units: gpm) in the NH during the summers of 2022.

4. Conclusions and discussion

Understanding atmospheric circulation changes has long relied on identifying recurring large-scale patterns (teleconnections). Historically, these teleconnections have been predominantly defined based on horizontal variables (e.g., geopotential height), which primarily capture the morphological or kinematic signatures of the circulation. In contrast, defining teleconnections from the perspective of vertical circulation intrinsically incorporates dynamic and thermodynamic mechanisms, as vertical motion is fundamentally tied to diabatic heating and adiabatic processes. Building upon this dynamical premise, this study establishes a three-dimensional analytical framework integrating the coupled vertical circulations. Notably, compared to traditional single-level height analyses (Zheng and Wang, 2019)—which sometimes yield moderate teleconnectivity (correlations around 0.5) and inter-pattern redundancies—our vertical stream function approach isolates highly significant (correlations around 0.74, Table S1,S2) and structurally

https://doi.org/10.5194/egusphere-2026-2824
Preprint. Discussion started: 16 June 2026
© Author(s) 2026. CC BY 4.0 License.

distinct linkages. This framework successfully unifies several major Northern Hemisphere (NH) teleconnections into a single, cohesive 3D system.

Specifically, utilizing the 3P-DGAC, 14 vertical teleconnection patterns (e.g., HCB, HCST, WWSJ) are identified in the mid-high latitudes, each characterized by counter-rotating vertical cells. The framework demonstrates robust validity over the 1979–2022 period, yielding mean spatial correlation coefficients of 0.64 and 0.60 for the reconstructed SAT and hemispheric circulation fields, respectively. Notably, during the extreme summer of 2022, a combination of dominant patterns captures over 75% of the regional SAT variance (peaking at 81.2% in southern China) and successfully reproduces the primary hemispheric circulation anomalies. These results suggest that the proposed 3D teleconnections effectively characterize the low-frequency atmospheric variability modulating the NH summer climate.

The robustness of this framework is deeply rooted in the physical reality that vertical circulation branches serve as critical conduits connecting horizontal wave trains with underlying surface forcings, including both thermal anomalies and topographic effects (Hoskins and Karoly, 1981). Existing studies provide solid evidence for this vertical-horizontal dynamical linkage. For example, He et al. (2018) demonstrated that overturning vertical circulations mediate the influence of sea-ice thermal forcing onto horizontal wave trains. Similarly, Peng et al., (2026) revealed that diabatic heating associated with extreme precipitation near Lake Baikal triggers meridional circulation anomalies, subsequently modulating large-scale wave processes.

While the present framework shows significant utility in diagnosing climate anomalies, several aspects warrant further investigation. First, the current analysis is constrained to seasonal-mean timescales, and some regional discrepancies in the reconstructed fields imply inherent complexities in circulation systems not fully captured by linear combinations. Future work should extend this 3D framework to daily or sub-seasonal scales to elucidate the transient eddy dynamics and weather-climate linkages driving compound extremes. Second, linking teleconnections explicitly with vertical circulation offers a novel perspective on the dynamical origins of wave trains. Future studies could employ the diagnostic methodologies developed in these references to quantitatively investigate how local temperature gradient anomalies excite these vertical circulation cells, thereby triggering and sustaining the coupled horizontal teleconnections (Hu et al., 2017, 2018a, b, 2020). Finally, incorporating these dynamically grounded 3D teleconnection indices into sub-seasonal to seasonal (S2S) prediction models or data-driven machine learning algorithms holds substantial potential for improving the forecasting skill of regional persistent heatwaves.

Code, data, or code and data availability

All the datasets used in this study are publicly available from the following websites: the ECMWF Reanalysis V5 dataset from https://cds.climate.copernicus.eu/cdsapp#!/search?type=dataset.

Data processing and analysis were carried out mainly using the Python scientific packages SciPy, NumPy, Pandas, and Xarray, while all visualizations were produced with Matplotlib and Cartopy.

https://doi.org/10.5194/egusphere-2026-2824
Preprint. Discussion started: 16 June 2026
© Author(s) 2026. CC BY 4.0 License.

Author contributions

H.Y. led the study, developed the research framework, performed the data analysis, and drafted the original manuscript. S.H. supervised the research, contributed to the study design, and revised the manuscript. J.P. assisted with data processing and contributed to the interpretation of results. W.Z. contributed to visualization and manuscript revision. Z.H. assisted with data collection and pre-processing. Y.W. contributed to discussion and manuscript editing. Z.Z. provided scientific guidance and contributed to manuscript revision. All authors discussed the results and contributed to the final manuscript.

Competing interests

The authors declare that there are no conflicts of interest.

Acknowledgements

We are grateful to G. Feng, J. Zhang, F. Ji, Q. Ma, D. Li, and C. Gao for their valuable suggestions. We thank J. Peng, B. Zhou, D. Li, J. Zhang, K. Wang, and L. Ma for improving the visualization. Additionally, we acknowledge S. Yan for her meticulous assistance in manuscript formatting and proofreading during the finalization of this paper. We thank for the technical support of the National Large Scientific and Technological Infrastructure “Earth System Numerical Simulation Facility” (https://cstr.cn/31134.02.EL).

Financial support

This work was supported by the Joint Funds of the National Natural Science Foundation of China(U2342205&U2342208), National Natural Science Foundation of China (42375063), Key Natural Science Foundation of Gansu Province (23JRRA1030) and the Fundamental Research Funds for the Central Universities of China (lzujbky-2024-it70).

https://doi.org/10.5194/egusphere-2026-2824
Preprint. Discussion started: 16 June 2026
© Author(s) 2026. CC BY 4.0 License.

REFERENCES

Affram, G., Zhang, W., Hari, V., Gao, S., Ratterman, C., Zhu, L., and Gillies, R. R.: Modulation of the pacific meridional mode on the dipole pattern of the CONUS summertime precipitation, Geophys. Res. Lett., 51, e2024GL109636, https://doi.org/10.1029/2024GL109636, 2024.

Barnston, A. G. and Livezey, R. E.: Classification, Seasonality and Persistence of Low-Frequency Atmospheric Circulation Patterns, Mon. Weather Rev., 115, 1083–1126, https://doi.org/10.1175/1520-0493(1987)115%253C1083:CSAPOL%253E2.0.CO;2, 1987.

Cassou, C., Terray, L., and Phillips, A. S.: Tropical Atlantic Influence on European Heat Waves, J. Clim., 18, 2805–2811, https://doi.org/10.1175/JCLI3506.1, 2005.

Chen, W., Hong, X., Lu, R., Jin, A., Jin, S., Nam, J.-C., Shin, J.-H., Goo, T.-Y., and Kim, B.-J.: Variation in summer surface air temperature over Northeast Asia and its associated circulation anomalies, Adv. Atmospheric Sci., 33, 1–9, https://doi.org/10.1007/s00376-015-5056-0, 2016.

Deng, K., Yang, S., Ting, M., Lin, A., and Wang, Z.: An Intensified Mode of Variability Modulating the Summer Heat Waves in Eastern Europe and Northern China, Geophys. Res. Lett., 45, 11,361-11,369, https://doi.org/10.1029/2018GL079836, 2018.

Deng, K., Yang, S., Ting, M., Zhao, P., and Wang, Z.: Dominant Modes of China Summer Heat Waves Driven by Global Sea Surface Temperature and Atmospheric Internal Variability, J. Clim., 32, 3761–3775, https://doi.org/10.1175/JCLI-D-18-0256.1, 2019.

Ding, Q. and Wang, B.: Circumglobal Teleconnection in the Northern Hemisphere Summer, J. Clim., 18, 3483–3505, https://doi.org/10.1175/JCLI3473.1, 2005.

Ding, Q., Wang, B., Wallace, J. M., and Branstator, G.: Tropical–Extratropical Teleconnections in Boreal Summer: Observed Interannual Variability, J. Clim., 24, 1878–1896, https://doi.org/10.1175/2011JCLI3621.1, 2011.

Enomoto, T., Hoskins, B. J., and Matsuda, Y.: The formation mechanism of the Bonin high in August, Q. J. R. Meteorol. Soc., 129, 157–178, https://doi.org/10.1256/qj.01.211, 2003.

Enomoto, T., Endo, H., Harada, Y., and Ohfuchi, W.: Relationship between High-Impact Weather Events in Japan and Propagation of Rossby Waves along the Asian Jet in July 2004, J. Meteorol. Soc. Jpn. Ser II, 87, 139–156, https://doi.org/10.2151/jmsj.87.139, 2009.

Folland, C. K., Knight, J., Linderholm, H. W., Fereday, D., Ineson, S., and Hurrell, J. W.: The summer north atlantic oscillation: past, present, and future, J. Clim., 22, 1082–1103, https://doi.org/10.1175/2008JCLI2459.1, 2009.

Fu, S., Zhu, Z., Yu, H., and Li, T.: The diversity of the boreal spring north atlantic sea surface temperature tripole pattern and corresponding northern hemispheric surface air temperature anomalies, Environ. Res. Lett., 20, 54043, https://doi.org/10.1088/1748-9326/adca47, 2025.

Fu, Z.-H., Zhou, W., Xie, S.-P., Zhang, R., and Wang, X.: Dynamic pathway linking Pakistan flooding to East Asian heatwaves, Sci. Adv., 2024.

He, S., Gao, Y., Furevik, T., Wang, H., and Li, F.: Teleconnection between sea ice in the barents sea in June and the silk road, pacific–japan and east asian rainfall patterns in August, Adv. Atmospheric Sci., 35, 52–64, https://doi.org/10.1007/s00376-017-7029-y, 2018.

Held, I. M. and Phillips, P. J.: A Barotropic Model of the Interaction between the Hadley Cell and a Rossby Wave, J. Atmospheric Sci., 47, 856–869, https://doi.org/10.1175/1520-0469(1990)047%253C0856:ABMOTI%253E2.0.CO;2, 1990.

https://doi.org/10.5194/egusphere-2026-2824
Preprint. Discussion started: 16 June 2026
© Author(s) 2026. CC BY 4.0 License.

Henley, B. J., Gergis, J., Karoly, D. J., Power, S., Kennedy, J., and Folland, C. K.: A tripole index for the interdecadal pacific oscillation, Clim. Dyn., 45, 3077–3090, https://doi.org/10.1007/s00382-015-2525-1, 2015.

Hersbach, H., Bell, B., Berrisford, P., Hirahara, S., Horányi, A., Muñoz-Sabater, J., Nicolas, J., Peubey, C., Radu, R., Schepers, D., Simmons, A., Soci, C., Abdalla, S., Abellan, X., Balsamo, G., Bechtold, P., Biavati, G., Bidlot, J., Bonavita, M., Chiara, G. D., Dahlgren, P., Dee, D., Diamantakis, M., Dragani, R., Flemming, J., Forbes, R., Fuentes, M., Geer, A., Haimberger, L., Healy, S., Hogan, R. J., Hólm, E., Janisková, M., Keeley, S., Laloyaux, P., Lopez, P., Lupu, C., Radnoti, G., Rosnay, P. de, Rozum, I., Vamborg, F., Villaume, S., and Thépaut, J.-N.: The ERA5 global reanalysis, Q. J. R. Meteorol. Soc., 146, 1999–2049, 2020.

Horel, J. D.: A Rotated Principal Component Analysis of the Interannual Variability of the Northern Hemisphere 500 mb Height Field, Mon. Weather Rev., 109, 2080–2092, https://doi.org/10.1175/1520-0493(1981)109%253C2080:ARPCAO%253E2.0.CO;2, 1981.

Hoskins, B. J. and Karoly, D. J.: The steady linear response of a spherical atmosphere to thermal and orographic forcing, J. Atmospheric Sci., 38, 1179–1196, https://doi.org/10.1175/1520-0469(1981)038%253C1179:TSLROA%253E2.0.CO;2, 1981.

Houze, R. A., Chen, S. S., Kingsmill, D. E., Serra, Y., and Yuter, S. E.: Convection over the Pacific Warm Pool in relation to the Atmospheric Kelvin-Rossby Wave*, J. Atmospheric Sci., 57, 3058–3089, https://doi.org/10.1175/1520-0469(2000)057%253C3058:COTPWP%253E2.0.CO;2, 2000.

Hu, S., Cheng, J., and Chou, J.: Novel three-pattern decomposition of global atmospheric circulation: generalization of traditional two-dimensional decomposition, Clim. Dyn., 49, 3573–3586, https://doi.org/10.1007/s00382-017-3530-3, 2017.

Hu, S., Chou, J., and Cheng, J.: Three-pattern decomposition of global atmospheric circulation: part I—decomposition model and theorems, Clim. Dyn., 50, 2355–2368, https://doi.org/10.1007/s00382-015-2818-4, 2018a.

Hu, S., Cheng, J., Xu, M., and Chou, J.: Three-pattern decomposition of global atmospheric circulation: part II—dynamical equations of horizontal, meridional and zonal circulations, Clim. Dyn., 50, 2673–2686, https://doi.org/10.1007/s00382-017-3763-1, 2018b.

Hu, S., Zhou, B., Gao, C., Xu, Z., Wang, Q., and Chou, J.: Theory of three-pattern decomposition of global atmospheric circulation, Sci. China Earth Sci., 63, 1248–1267, https://doi.org/10.1007/s11430-019-9614-y, 2020.

Huang, H., Zhu, Z., and Li, J.: Disentangling the unprecedented yangtze river basin extreme high temperatures in summer 2022: combined impacts of the reintensified La niña and strong positive NAO, J. Clim., 37, 927–942, https://doi.org/10.1175/JCLI-D-23-0466.1, 2024.

Kiladis, G. N.: Observations of Rossby Waves Linked to Convection over the Eastern Tropical Pacific, J. Atmospheric Sci., 55, 321–339, https://doi.org/10.1175/1520-0469(1998)055%253C0321:OORWLT%253E2.0.CO;2, 1998.

Kosaka, Y. and Nakamura, H.: Structure and dynamics of the summertime Pacific–Japan teleconnection pattern, Q. J. R. Meteorol. Soc., 132, 2009–2030, https://doi.org/10.1256/qj.05.204, 2006.

Lembo, V., Bordoni, S., Bevacqua, E., Domeisen, D. I. V., Franzke, C. L. E., Galfi, V. M., Garfinkel, C., Grams, C. I., Hochman, A., Jha, R., Kornhuber, K., Kwasniok, F., Lucarini, V., Messori, G., Pappert, D., Perez-Fernandez, I., Riboldi, J., Russo, E., Shaw, T. A., Strigunova, I., Strnad, F., Yiou, P., and Zagar, N.: Dynamics, statistics and predictability of Rossby waves, heatwaves and spatially compounded extreme events, Bull. Am. Meteorol. Soc., https://doi.org/10.1175/BAMS-D-24-0145.1, 2024.

Li, J. and Ruan, C.: The North Atlantic–Eurasian teleconnection in summer and its effects on Eurasian climates, Environ. Res. Lett., 13, 024007, https://doi.org/10.1088/1748-9326/aa9d33, 2018.

https://doi.org/10.5194/egusphere-2026-2824
Preprint. Discussion started: 16 June 2026
© Author(s) 2026. CC BY 4.0 License.

Li, J., Zheng, F., Sun, C., Feng, J., and Wang, J.: Pathways of Influence of the Northern Hemisphere Mid-high Latitudes on East Asian Climate: A Review, Adv. Atmospheric Sci., 36, 902–921, https://doi.org/10.1007/s00376-019-8236-5, 2019.

Li, X., Lu, R., and Ahn, J.-B.: Combined Effects of the British–Baikal Corridor Pattern and the Silk Road Pattern on Eurasian Surface Air Temperatures in Summer, J. Clim., 34, 3707–3720, https://doi.org/10.1175/JCLI-D-20-0325.1, 2021.

Liu, X., Zhu, Z., Lu, R., Miao, Z., Li, W., and Hsu, P.: Unprecedented july rainfall in north China in 2021: combined effect of atlantic warming and arctic sea-ice loss, J. Geophys. Res. Atmospheres, 128, e2022JD038068, https://doi.org/10.1029/2022JD038068, 2023.

Liu, Z. and Alexander, M.: Atmospheric bridge, oceanic tunnel, and global climatic teleconnections, Rev. Geophys., 45, 2005RG000172, https://doi.org/10.1029/2005RG000172, 2007.

Lu, R. and Lin, Z.: Role of Subtropical Precipitation Anomalies in Maintaining the Summertime Meridional Teleconnection over the Western North Pacific and East Asia, J. Clim., 22, 2058–2072, https://doi.org/10.1175/2008JCLI2444.1, 2009.

Lu, R.-Y., Oh, J.-H., and Kim, B.-J.: A teleconnection pattern in upper-level meridional wind over the north african and eurasian continent in summer, Tellus Dyn. Meteorol. Oceanogr., 54, 44, https://doi.org/10.3402/tellusa.v54i1.12122, 2002.

Nitta, T.: Convective activities in the tropical western pacific and their impact on the northern hemisphere summer circulation, J. Meteorol. Soc. Jpn. Ser II, 65, 373–390, https://doi.org/10.2151/jmsj1965.65.3_373, 1987.

Pendergrass, A. G. and Gerber, E. P.: The rain is askew: two idealized models relating vertical velocity and precipitation distributions in a warming world, J. Clim., 29, 6445–6462, https://doi.org/10.1175/JCLI-D-16-0097.1, 2016.

Peng, J., Hu, S., Jing, Z., Guan, Y., Zhao, Y., Liu, Y., and Zheng, Z.: Ripple effects of extreme precipitation in the northern baikal region on concurrent extreme heat events, Clim. Dyn., 64, 221, https://doi.org/10.1007/s00382-026-08194-0, 2026.

Sardeshmukh, P. D., Compo, G. P., and Penland, C.: Need for caution in interpreting extreme weather statistics, J. Clim., 28, 9166–9187, https://doi.org/10.1175/JCLI-D-15-0020.1, 2015.

Schubert, S., Wang, H., and Suarez, M.: Warm season subseasonal variability and climate extremes in the northern hemisphere: the role of stationary rossby waves, J. Clim., 24, 4773–4792, https://doi.org/10.1175/JCLI-D-10-05035.1, 2011.

Schubert, S. D., Wang, H., Koster, R. D., Suarez, M. J., and Groisman, P. Ya.: Northern eurasian heat waves and droughts, J. Clim., 27, 3169–3207, https://doi.org/10.1175/JCLI-D-13-00360.1, 2014.

Tamarin-Brodsky, T. and Hadas, O.: The asymmetry of vertical velocity in current and future climate, Geophys. Res. Lett., 46, 374–382, https://doi.org/10.1029/2018GL080363, 2019.

Tang, S., Qiao, S., Wang, B., Liu, F., Feng, T., Yang, J., He, M., Chen, D., Cheng, J., Feng, G., and Dong, W.: Linkages of unprecedented 2022 Yangtze River Valley heatwaves to Pakistan flood and triple-dip La Niña, Npj Clim. Atmospheric Sci., 6, 44, https://doi.org/10.1038/s41612-023-00386-3, 2023.

Taylor, A. H., Jordan, M. B., and Stephens, J. A.: Gulf Stream shifts following ENSO events, Nature, 393, 638–638, https://doi.org/10.1038/31380, 1998.

https://doi.org/10.5194/egusphere-2026-2824
Preprint. Discussion started: 16 June 2026
© Author(s) 2026. CC BY 4.0 License.

Thakur, A. B. S., Sukhatme, J., and Harnik, N.: Investigating the role of tropical and extratropical waves in the hadley circulation via present-day earth-like to globally uniform sea-surface temperature forcing, Q. J. R. Meteorol. Soc., 150, 3578–3600, https://doi.org/10.1002/qj.4784, 2024.

Thompson, V., Dunstone, N. J., Scaife, A. A., Smith, D. M., Hardiman, S. C., Ren, H.-L., Lu, B., and Belcher, S. E.: Risk and dynamics of unprecedented hot months in South East China, Clim. Dyn., 52, 2585–2596, https://doi.org/10.1007/s00382-018-4281-5, 2019.

Wallace, J. M. and Gutzler, D. S.: Teleconnections in the geopotential height field during the northern hemisphere winter, Mon. Weather Rev., 109, 784–812, https://doi.org/10.1175/1520-0493(1981)109%253C0784:TITGHF%253E2.0.CO;2, 1981.

Wang, C., Zheng, J., Lin, W., and Wang, Y.: Unprecedented Heatwave in Western North America during Late June of 2021: Roles of Atmospheric Circulation and Global Warming, Adv. Atmospheric Sci., 1–15, https://doi.org/10.1007/s00376-022-2078-2, 2022.

Wang, L., Wang, C., and Guo, D.: Evolution mechanism of synoptic-scale EAP teleconnection pattern and its relationship to summer precipitation in China, Atmospheric Res., 214, 150–162, https://doi.org/10.1016/j.atmosres.2018.07.023, 2018.

Wang, Y., Zhou, W., and Wang, C.: Physical mechanism of the rapid increase in intense and long-lived extreme heatwaves in the Northern Hemisphere since 1980, Sci. China Earth Sci., https://doi.org/10.1007/s11430-023-1332-x, 2024.

Wu, R.: A mid-latitude Asian circulation anomaly pattern in boreal summer and its connection with the Indian and East Asian summer monsoons, Int. J. Climatol., 22, 1879–1895, https://doi.org/10.1002/joc.845, 2002.

Wulff, C. O., Greatbatch, R. J., Domeisen, D. I. V., Gollan, G., and Hansen, F.: Tropical Forcing of the Summer East Atlantic Pattern, Geophys. Res. Lett., 44, 11,166-11,173, https://doi.org/10.1002/2017GL075493, 2017.

Xu, K., Lu, R., Mao, J., and Chen, R.: Circulation anomalies in the mid–high latitudes responsible for the extremely hot summer of 2018 over northeast Asia, Atmospheric Ocean. Sci. Lett., 12, 231–237, https://doi.org/10.1080/16742834.2019.1617626, 2019a.

Xu, P., Wang, L., and Chen, W.: The british–baikal corridor: a teleconnection pattern along the summertime polar front jet over eurasia, J. Clim., 32, 877–896, https://doi.org/10.1175/JCLI-D-18-0343.1, 2019b.

Xu, P., Wang, L., Liu, Y., Chen, W., and Huang, P.: The record-breaking heat wave of June 2019 in Central Europe, Atmospheric Sci. Lett., 21, e964, https://doi.org/10.1002/asl.964, 2020.

Xu, P., Wang, L., Dong, Z., Li, Y., Shen, X., and Chen, W.: The British–Okhotsk Corridor Pattern and Its Linkage to the Silk Road Pattern, J. Clim., 35, 5787–5804, https://doi.org/10.1175/JCLI-D-21-0705.1, 2022.

Yasunari, T. J., Nakamura, H., Kim, K.-M., Choi, N., Lee, M.-I., Tachibana, Y., and Da Silva, A. M.: Relationship between circum-Arctic atmospheric wave patterns and large-scale wildfires in boreal summer, Environ. Res. Lett., 16, 064009, https://doi.org/10.1088/1748-9326/abf7ef, 2021.

Zhang, X., Zhou, T., Zhang, W., Ren, L., Jiang, J., Hu, S., Zuo, M., Zhang, L., and Man, W.: Increased impact of heat domes on 2021-like heat extremes in North America under global warming, Nat. Commun., 14, 1690, https://doi.org/10.1038/s41467-023-37309-y, 2023.

Zheng, J. and Wang, C.: Hot Summers in the Northern Hemisphere, Geophys. Res. Lett., 46, 10891–10900, https://doi.org/10.1029/2019GL084219, 2019.

https://doi.org/10.5194/egusphere-2026-2824
Preprint. Discussion started: 16 June 2026
© Author(s) 2026. CC BY 4.0 License.

Zhu, Z. and Li, T.: A New Paradigm for Continental U.S. Summer Rainfall Variability: Asia–North America Teleconnection, J. Clim., 29, 7313–7327, https://doi.org/10.1175/JCLI-D-16-0137.1, 2016.

Zhu, Z., Zhou, Y., Jiang, W., Fu, S., and Hsu, P.: Influence of compound zonal displacements of the south Asia high and the western pacific subtropical high on meiyu intraseasonal variation, Clim. Dyn., 61, 3309–3325, https://doi.org/10.1007/s00382-023-06726-6, 2023.